Geophysical Research Letters

Supporting Information for

Biologically Induced Changes in thse Partitioning of Submicron Particulates Between Bulk Seawater and the Sea Surface Microlayer

Daniel R. Crocker[*,1], Grant B. Deane[2], Ruochen Cao[1], Mitchell V. Santander[1], Clare K. Morris[2], Brock A. Mitts[1], Julie Dinasquet[2], Sarah Amiri[1], Francesca Malfatti[2,3,4], Kimberly A. Prather[1,2], Mark H. Thiemens[1]

[1]Department of Chemistry and Biochemistry, University of California, San Diego, La Jolla, California, 92093, USA

[2]Scripps Institution of Oceanography, University of California, San Diego, La Jolla, California, 92037, USA

[3]University of Trieste, Trieste 34100, Italy
[4]OGS (Istituto Nazionale di Oceanografia e di Geofisica Sperimentale), Trieste 34100, Italy

Contents of this file

Introduction

The Supporting Information contains three text sections, four figures, and two tables. The text sections include: a description of mesocosm Experiment 2 where minimal phytoplankton growth occurred (Text S1), measurements of chlorophyll-a (chl-a); bacteria; viruses; and TEP (Text S2), and details on software analysis of the particulate size distributions (Text S3). Figure S1 displays the progression of chl-a, bacteria, virus, and SMP concentrations throughout Experiment 2. Figure S2 shows the seawater temperature throughout Experiments 1 and 2. Figure S3 displays the phytoplankton community composition during Experiment 1. Figure S4

shows a correlation plot between SSML TEP concentrations and 0.4-0.7 μm SSML particulates in Experiment 1. Tables S1 and S2 give the Pearson correlations between SMP size fractions and biological variables for Experiments 1 and 2, respectively.

Text 1. Microbial Activity during Experiment 2

Throughout the entirety of Experiment 2 very little phytoplankton growth (chl-a) was observed and chl-a values remained similar to the Experiment 1 pre-bloom values. Despite the lack of an exponential phytoplankton growth or decay phase, we include a brief description of Experiment 2 here to demonstrate the importance of the complete microbial loop on microbial mode growth. At the beginning of the Experiment 2, the bacteria and virus concentrations increased, but bacteria concentrations only correlated with the smallest particulate size fraction (0.4-0.55 μm, r=0.80), and viruses did not correlate with any of the SMP size fractions (Table S2). The smaller bacteria sizes observed in Experiment 2 are likely due to the lack of significant primary productivity, an important food source for bacteria proliferation (Palumbo et al., 1984). With most bacteria sizes in the 0.4-0.55 μm range, it follows that viral lysis likely produced particulates below 0.4 μm (Shibata et al., 1997). These particulates would be outside our measured size range, explaining the lack of correlation between microbial mode SMPs and virus concentrations in Experiment 2. We point out these observations from Experiment 2 to illustrate that growth of microbial mode SMPs is dependent on the interactions between multiple components of the microbial loop: phytoplankton, bacteria, and viruses (Azam et al., 1983). Notably, atmospheric studies have found that the organic composition of SSA is also influenced by interactions between multiple components of the microbial loop (O'Dowd et al., 2015; Wang

et al., 2015), and chl-alone cannot explain the enrichment of organic matter in SSA (Fuentes et al., 2010; Quinn et al., 2014; Rinaldi et al., 2013). Given these parallels, future studies may be useful to determine the extent to which biologically induced changes in seawater SMP concentrations and distributions impact the composition of SSA.

Text S2. Chl-a, Phytoplankton, Bacteria, Virus, and TEP Measurements

During the mesocosm experiments, a homemade, continuous flow system provided a continuous time series of chl-a concentration in the wave channel. This system employed a Sea Bird Scientific ECO-Triplet-BBFL2 sensor to measure chl-a using fluorescence at excitation/emission wavelengths of 470/695 nm. The *in situ* chl-a values were calibrated using measurements of extracted chl-a taken from the bulk seawater and analyzed fluorometrically according to CALCOFI methods (Holm-Hansen et al., 1965).

For bacteria and virus quantification, bulk seawater samples were prepared according to standard protocols (Brussaard, 2004; Gasol & Del Giorgio, 2000; Marie et al., 1997). All samples were preserved with 5% glutaraldehyde, flash frozen with liquid nitrogen, and stored at -80˚C (Noble & Fuhrman, 1998). Bacteria samples were diluted 10-fold in 1x TE buffer at pH 8 and stained for 10 minutes with SYBR Green I in the dark at room temperature (Gasol & Del Giorgio, 2000). Virus samples were diluted 50-fold in 1x TE buffer at pH 8 and stained for 10 minutes with SYBR Green I at 80˚C in the dark (Brussaard, 2004). Finally, enumeration of bacteria and viruses was carried out using a BD FACSCanto II™ flow cytometer.

Transparent exopolymer particulates (TEP) were measured following the colorimetric method as described by Engel (2009). After storage at -20°C, SSML samples were filtered onto 0.4 µm polycarbonate filters (Pall Corp.) and stained with Alcian Blue (0.02%). The Alcian Blue

was then released with 80% sulfuric acid over a 4-hour incubation at 4°C and absorbance was measured at 787 nm. TEP concentrations were determined following a calibration with Xanthan Gum standards and blank controls with pure water and filtered seawater.

Text S3. MANTA Software Analysis of Particulate Sizes

The MANTA Viewsizer® 3000 uses three lasers, blue (450 nm), green (532 nm), and red (635 nm), to illuminate particulates in a sample of seawater (Singh et al., 2019). Light scattered by particulates in a 2.5 µL viewfield of the sample is projected on a charged-coupled device (CCD) array and spectrally resolved to provide an image for each spectral band. A sequence of these images is recorded and saved to the computer as a video file. For these experiments, 100 videos were taken for each sample to ensure that enough particulates were identified to obtain an accurate size distribution. Analysis software identifies each individual particulate in an image and tracks its Brownian motion through the seawater medium in subsequent images. For each individual particulate, the mean square displacement is determined from the sequence of images and used to calculate the diffusion coefficient (D). The hydrodynamic diameter (d_h) of the particulate can then be calculated by the software using the Stokes-Einstein equation (see Equation 1 in Section 2.3.1 of the main text). The particulate sizes reported by the software were organized into 0.1 µm bin widths starting from a bin midpoint diameter of 0.405 µm up to 0.995 µm.

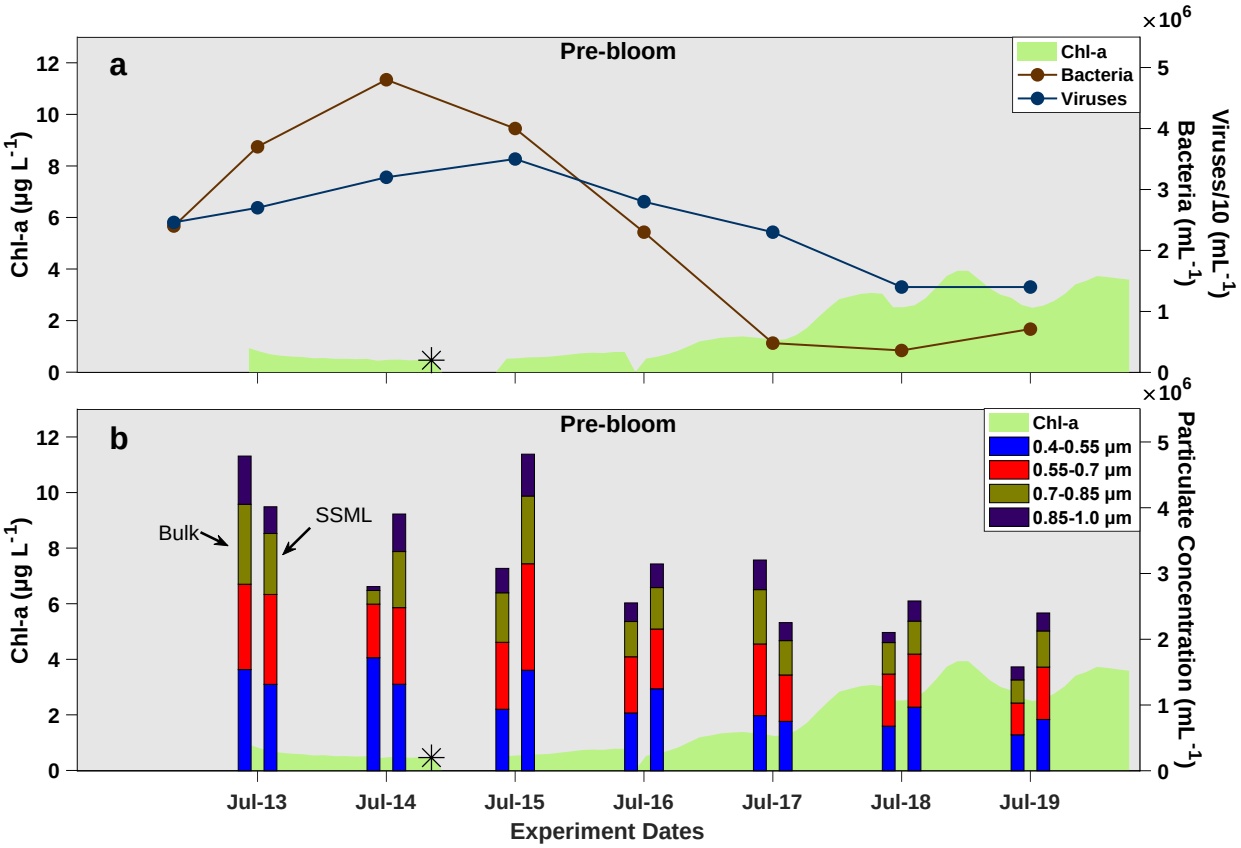

Figure S1. a) Development of chl-a, bacteria, and virus concentrations throughout Experiment 2. In Experiment 2, the biological progression was different from Experiment 1 with bacteria and virus concentrations increasing before algae growth nutrients were added (asterisk). **b)** The particulate concentrations for the bulk (left bars) and SSML (right bars) in Experiment 2 with stacked bars displaying SMP concentrations for equally spaced 0.15 µm size bins. Experiment 2 lacked exponential phytoplankton growth and decay periods and only exhibited a pre-bloom phase with similar chl-a concentrations to the Experiment 1 pre-bloom phase (Figure 2a).

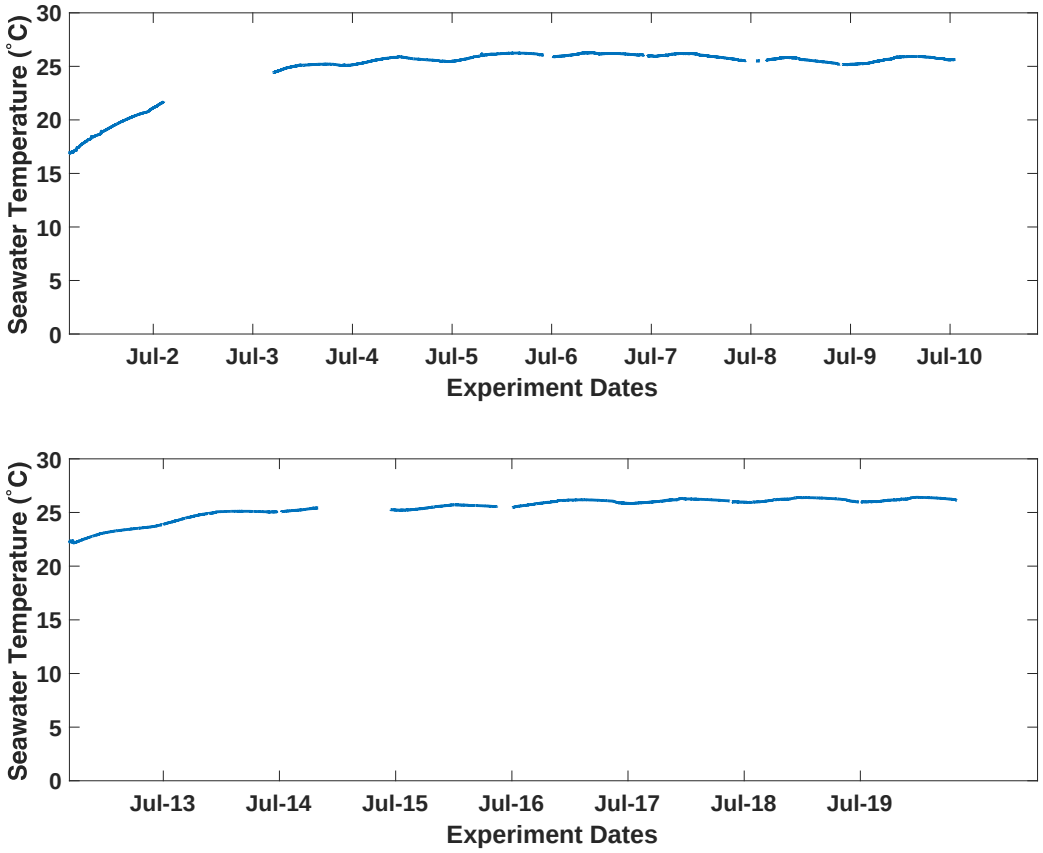

Figure S2. Time series of the seawater temperature throughout Experiment 1 (top) and Experiment 2 (bottom). Both experiments started with the lower temperature of the ambient coastal seawater and gradually warmed to around 25 ˚C, the temperature inside the Hydraulics Laboratory where the wave channel experiments were conducted.

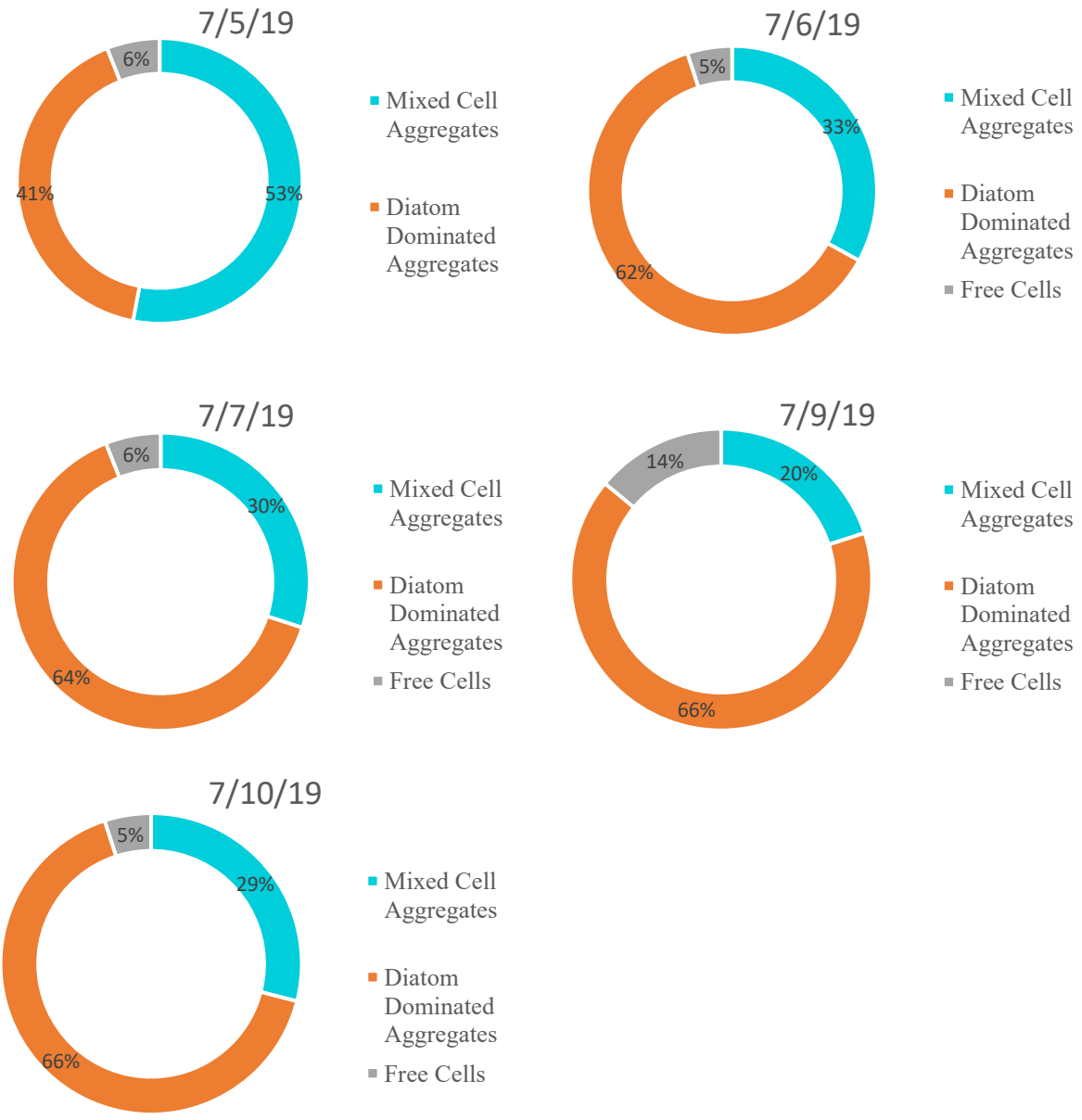

Figure S3. Daily community composition of phytoplankton in the bulk seawater for Experiment 1. The community shifts from a majority of mixed cell aggregates one day after nutrient addition to mostly diatom dominated aggregates in the growth and decay phases.

Table S1. Pearson correlation coefficients for Experiment 1 bulk SMPs and biological variables

Experiment 1	0.4-0.55 µm Bulk	0.55-0.7 µm Bulk	0.7-0.85 µm Bulk	0.85-1.0 µm Bulk	Chl-a	Bacteria	Virus
0.4-0.55 µm Bulk	1.00	**0.89**[a]	**0.77**	**0.74**	0.65	0.64	**0.83**
0.55-0.7 µm Bulk	--	1.00	**0.97**	**0.95**	**0.75**	**0.76**	0.58
0.7-0.85 µm Bulk	--	--	1.00	**0.99**	**0.83**	**0.74**	0.42
0.85-1.0 µm Bulk	--	--	--	1.00	**0.80**	0.68	0.38
Chl-a	--	--	--	--	1.00	0.61	0.50
Bacteria	--	--	--	--	--	1.00	0.41
Virus	--	--	--	--	--	--	1.00

[a] Coefficients (lower)higher than (-)0.7 are listed in bold and considered strong correlations (Moore et al., 2013)

Table S2. Pearson correlation coefficients for Experiment 2 bulk SMPs and biological variables

Experiment 2	0.4-0.55 µm Bulk	0.55-0.7 µm Bulk	0.7-0.85 µm Bulk	0.85-1.0 µm Bulk	Chl-a	Bacteria	Virus
0.4-0.55 µm Bulk	1.00	0.50	0.18	0.21	-0.66	**0.83**[a]	0.65
0.55-0.7 µm Bulk	--	1.00	**0.87**	**0.83**	-0.57	0.37	0.53
0.7-0.85 µm Bulk	--	--	1.00	**0.98**	-0.23	0.09	0.22
0.85-1.0 µm Bulk	--	--	--	1.00	-0.24	0.12	0.23
Chl-a	--	--	--	--	1.00	**-0.79**	**-0.98**
Bacteria	--	--	--	--	--	1.00	**0.85**
Virus	--	--	--	--	--	--	1.00

[a] Coefficients (lower)higher than (-)0.7 are listed in bold and considered strong correlations (Moore et al., 2013)

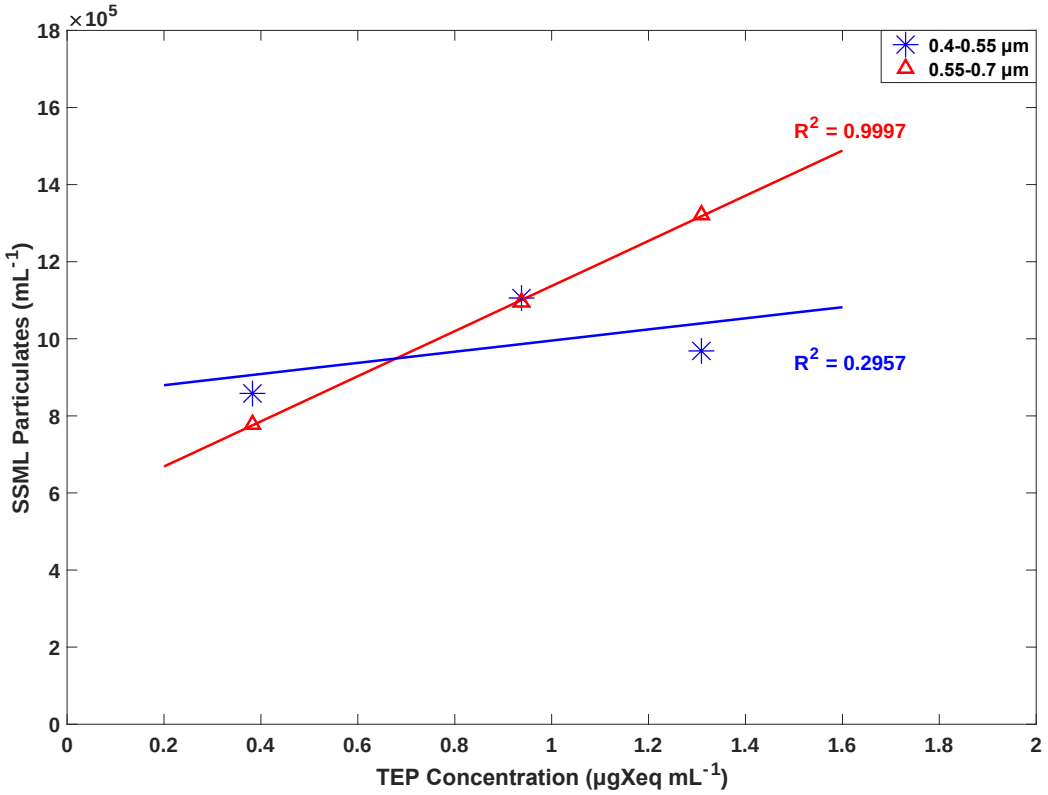

Figure S4. Plot of the SSML TEP (>0.4 µm) concentration, reported in µg of Xanthan Gum equivalents mL^{-1}, versus the concentration of 0.4-0.55 and 0.55-0.7 µm SSML particulates for samples measured on 7/6, 7/7, and 7/9. For these measurements there is a very strong correlation between the amount of TEP in the SSML and the concentration of 0.55-0.7 µm microbial mode particulates. The largest TEP concentration occurs on 7/7, the day with peak chl-a and bacteria concentrations.